Biologia (2023) 78:2779–2791
https://doi.org/10.1007/s11756-023-01402-w

ORIGINAL ARTICLE

Let us go back to the type materials to investigate the cranial differences among the *Meriones* species (Rodentia, Gerbillinae)

Fatemeh Tabatabaei Yazdi[1] · **Sarina Dousti**[1]

Received: 25 November 2022 / Accepted: 24 March 2023 / Published online: 2 May 2023

Abstract

The genus *Meriones* Illiger, 1811 comprises species that are mainly desert or semi-desert inhabitants in the Palearctic region. These species are usually distinguished from each other by some external and cranial characters, yet they show a considerable level of intra-specific variation. Studies demonstrated that their taxonomy is complex, and that they show a considerable level of morphological plasticity. This study mainly deals with such taxonomical issues in jirds belonging to the genus *Meriones*, and provides a contribution to their conservation status. To explore cranial shape and size differences among *Meriones* species, morphological variables of type specimens of ten valid *Meriones* species, as well as of their synonyms were investigated. These include *Meriones libycus*, *M. crassus, M. persicus, M. tristrami, M. meridianus, M. hurrianae, M. rex, M. shawii, M. sacramenti*, and *M. arimalius*. To obtain the geometry of the biological forms, 2D-landmark data was acquisitioned, and analysed using geometric morphometric techniques. Multivariate analyses on the shape data of ventral, dorsal, and lateral views showed that, although some species reveal an overlap in morpho-space, in some views they are morphologically distinct. A cluster analyses demonstrates the existence of at least two major groups. Although, it is possible to discriminate some *Meriones* species based on the relative bulla' size, the results support the hypothesis that this criterion is not applicable to all of them. Size analyses demonstrated that the inter-landmarks distances representing the length of the tooth row and the opening of suprameatal triangle are significantly different between some jird species, and hence should be considered as a distinctive trait in the identification keys on jirds. Conclusively, only a thorough systematic revision of the genus *Meriones*, considering zoogeographic and ecological data, may complete the puzzle of the taxonomy of these species.

Keywords Biodiversity · Geometric morphometrics · Mammals · Morphology · Taxonomy

Introduction

Species diversity is one of the most important and common aspects of biodiversity as a whole (Mahmoodzadeh et al. 2022). To achieve an effective conservation of species diversity, an integrative approach of species identification and recording is needed. The genus *Meriones* Illiger, 1811, contains 16 species, most of them referred to as jirds. They are widespread in the Palearctic region (North Africa to the Far East), especially in the Middle East and Central Asia (Wilson and Reeder 2005; Darvish 2011; Stoetzel et al. 2017). These species show adaptation to aridity in physiological and morphological characteristics. Well-developed tympanic bulla is remarkable in these species (Pavlinov and Rogovin 2000; Pavlinov 2008; Tabatabaei Yazdi et al. 2014; Alhajeri et al. 2015). Most ecological aspects of *Meriones* species are still poorly known, and the taxonomy of these rodents is muddled, especially for the species complexes (Chaworth-Musters and Ellerman 1947; Chevret and Dobigny 2005; Wilson and Reeder 2005; Darvish 2009, 2011; Tabatabaei Yazdi et al. 2012).

The identification key of jirds mainly focuses on bulla inflation (Ellerman 1948; Pavlinov 2008). Previously, Tabatabaei Yazdi (2011) and Tabatabaei Yazdi et al. (2012, 2014), clearly mentioned that a "more swollen bulla" and "open/closed suprameatal triangle" are not appropriate criteria and thus not applicable for the identification of some taxa (i.e., *M. c. longifrons* and *M. c. charon*).

✉ Fatemeh Tabatabaei Yazdi
f.tabatabaei@um.ac.ir

[1] Environment Department, Faculty of Natural Resources and Environment, Ferdowsi University of Mashhad, Azadi Sq., Mashhad, Iran

Holotypes are a crucial source of reference material for biologists focusing on comparative studies, especially in taxonomy. However, type materials do not represent the mean shape of the taxon, ideally, a type specimen exemplifies the essential characteristics of a taxon to which it belongs. Thus, in this study, using geometric morphometric methods, we have investigated the morphological and size differences among the holotypes.

Recently, Chevret and Dobigny (2005), Yigit et al. (2006), Pavlinove (2008), Darvish (2011), Tabatabaei Yazdi and Adriaens (2013), and Dianat et al. (2020), using different techniques reviewed the systematic relationships among some jird species. However, their results are not sufficient to fill the gap required for a modern systematic revision of *Meriones*. Thus, in this article, we focus on the taxa with mix-up taxonomy, limited distribution range, and overlapped distribution with close taxa. By using geometric morphometrics, we explored to what degree type specimens can allow showing the interspecies cranial shape and size differences, and what that infers in the context of taxonomy and biodiversity conservation.

Material and methods

Specimens collection

A total of 37 holotypes were investigated. The studied species are reference specimens of each taxon. Those belong to *Meriones libycus* (including *M. arimalius*), *M. crassus, M. persicus, M. tristrami, M. meridianus, M. hurrianae, M. rex, M. shawii, M. sacramenti*, and *Sekeetamys calurus* (Musser and Carleton 2005). In the previous phylogenetic reconstructions, *S. calurus* (a basal species of *Meriones*) is included in the genus *Meriones* (Wrobel 2006).

Distribution range and type localities of the studied species are as follows (Darvish 2011; Musser and Carleton 2005; Yigit et al. 2006; Tabatabaei Yazdi 2017):

Sundevall's Jird, *Meriones crassus* Sundevall, 1842

Type locality: Egypt, Sinai, Fount of Moses (Ain Musa). Distribution: Across North Africa from Morocco through Niger, Sudan, and Egypt to Israel, Jordan, Syria, SE Anatolia (Turkey), Saudi Arabia, Iraq, Iran, Afghanistan, and southern Turkmenistan.

Libyan Jird, *Meriones libycus* Lichtenstein, 1823

Type locality: Egypt, near Alexandria, Libyan Desert. Distribution: North Africa from Western Sahara (Rio de Oro) to Egypt, from Arabia to the Iranian Plateau, and Turkmenistan to Sinkiang in W China.

Persian Jird, *Meriones persicus* Blanford, 1875

Type locality: Iran, Kohrud, 72 miles N. of Isfahan, Iran. Distribution: Eastern Minor Asia and Transcaucasia through NE Iraq and Iran, to south Western Turkmenistan, Afghanistan, and Pakistan (West of Indus River).

Shawi's Jird, *Meriones shawii* (Dovernoy, 1842)

Type locality: Algeria, Oman. Distribution: Mediterranean littoral from E Morocco through N Algeria, Tunisia, Libya, and Egypt to N Sinai.

King Jird, *Meriones rex* Yerbury and Thomas, 1895

Type locality: Yemen, Lahej, near Aden. Distribution: Yemen highlands in SW Arabian Peninsula, from Mecca in Saudi Arabia to near Aden.

Tristram's Jird, *Meriones tristrami* Thomas, 1892

Type locality: Dead Sea area, Palestine. Distribution: from Arabian Peninsula to Asia Minor, From Israel, Lebanon, and Jordan to E Turkey, Syria, N Iraq, Transcaucasia and NW Iran.

Boxton's Jird, *Meriones sacramenti* Thomas, 1922

Type locality: Israel, 10 mi S Birsheba. Distribution: A small range in Israel (on the coastal plain south of the Yarqon River and in the N Negev) and NE Sinai Peninsula of Egypt.

Indian desert Jerbil, *Meriones hurrianae* Jordan, 1867

Type locality: India, Hurriana district. Distribution: Semi-desert from Punjab and Kathiawar to S. Afghanistan, and S.E. Iran.

Midday Jird, *Meriones meridianus* (Pallas, 1773)

Type locality: South East Russia, Astrakhanskaya Oblast, Dosang. Distribution: From Lower Don River and north of the Caucasus to Mongolia and N China, South to East Turkey, E Iran, and N Afghanistan.

Bushy-tailed Jird, *Sekeetamys calurus* (Thomas, 1892)

Type locality: Egypt, Sinai, near Tor. Distribution: Restricted to rocky and cliff habitat from E Egypt (east side of the Nile) through Sinai, SE Israel, and SW Jordan into Saudi Arabia. Although researchers now agree that *calurus* merits generic separation, previously, it has been assigned to the genus *Meriones* (Wilson and Reeder 2005).

All the studied materials are intact skulls of type, co-type, lectotype, and paralectotype specimens gathered at the collections of the British Natural History Museum (London, UK). In order to be able to assign the specimens to nominal taxa, we followed the taxonomy used by the museums. For their nominal taxa, and the synonyms, collection numbers and the collected locality, see Table 1. For information about the collection number of studied species, see Appendix.

Geometric morphometric methods

Geometric morphometrics is a valuable tool for exploring inter-specific shape differences. This technique has a considerable potential for taxonomic identification (Bookstein 1991; Rohlf 1996; Fadda and Corti 2001; Zelditch et al. 2004; Cardini et al. 2007; Macholán et al. 2008; Cardini and Elton 2009; Abiadh et al. 2010; Cardini et al.

Table 1 Studied taxa and current scientific names, including collection numbers at British Museum of Natural History (Wilson and Reeder 2005)

Taxon	Synonym	Type locality	Museum No.
M. c. pallidus	*M. crassus*	Sudan, Atbara	19. 8. 16. 11.
M. charon Thomas, 1919	*M. crassus*	Iran, Khuzestan, Ahwaz	5. 10. 4. 38
M. ismahelis Cheesman and Hinton, 1924	*M. crassus*	Arabia, Hufuf	24. 8. 2. 4
M. pelerinus Thomas, 1919	*M. crassus*	Arabia, Tebuk	10. 3. 12. 5
M. palidus tripolius Thomas, 1919	*M. crassus*	Libya, Gebel Limhersuk	2. 11. 4. 64
M. longifrons Lataste, 1884	*M. crassus*	Arabia, Jeddah	83. 11. 30. 1
M. longifrons Lataste, 1884	*M. crassus*	Arabia, Jeddah	19. 7. 7. 2246
M. arimalius Cheesman and Hinton, 1924	*M. libycus*	Saudi Arabia, Yabrin (Jabrin), Djebel Agoula	24. 8. 2. 5.
M. erythrourus aquilo	*M. libycus*	One hundred miles of Gutschen, Zungaria, Chinese central Asia	12. 4. 1. 44.
M. gaetulus Lataste, 1882	*M. libycus*	Algeria	82. 7. 29. 9
M. l. caudatus Thomas, 1919	*M. libycus*	Libya, Tripolitania, Bir Fredjan	2. 11. 4. 56
M. schousboeii tuareg Thomas, 1925	*M. libycus*	West Africa	25. 5. 12. 59
M. schousboeii Loche, 1867	*M. libycus*	Southern Algeria	19. 7. 7. 1560
M. syrius Thomas, 1919	*M. libycus*	Syria, Karyatein, Syrian Desert	5. 7. 2. 2
M. s. edithae Cheesman and Hinton, 1924	*M. libycus*	Arabia, Hufuf, Khudud Spring	24. 8. 2. 6.
M. s. evelynae Cheesman and Hinton, 1924	*M. libycus*	Arabia, Hufuf, Khorassan Spring	24. 8. 2. 7.
M. ambrosius Thomas, 1919	*M. persicus*	North east of Ahwaz, Persia into Baluchistan.	5. 10. 4. 35
M. p. persicus (Blanford, 1875)	*M. persicus*	Iran, Kohrud, north of Isfahan.	76. 3. 10. 2
M. p. baptistae Thomas, 1920	*M. persicus*	Pasht Kuh, Bluchistan.	19. 11. 7. 69.
M. auratus (Duvernoy, 1842)	*M. shawii*	Northern Syria	19. 7. 7. 1567
M. albipes Lataste, 1882	*M. shawii*	Msila, Algeria.	82. 7. 29. 10.
M. auziensis Lataste, 1882	*M. shawii*	Ouedakarit, near Aumale, Algeria.	82. 7. 29. 8.
M. isis Thomas, 1919	*M. shawii*	Ramleh, near Alexandria, Egypt.	92. 7. 1. 6
M. s. crassibulla Lataste, 1885	*M. shawii*	Tebessa, Algeria.	19. 7. 7. 2981
M. s. longiceps Lataste, 1885	*M. shawii*	Bordeaux, Tunis.	19. 7. 7. 1941
M. trouessarti Lataste, 1882	*M. shawii*	Algeria	82. 7. 29. 7.
M. buryi Thomas, 1902	*M. rex*	Zabed, Haushabi, in hills north of Aden, southern Arabia.	2. 11. 22. 9
Tatera philbyi Morrison-Scott, 1939	*M. rex*	Najran, Arabia.	40. 272
M. rex Yerbury and Thomas, 1895	*M. rex*	Yemen, Lahej, near Aden.	95. 6. 1. 30
M. blackleri Thomas, 1903	*M. tristrami*	Western Asia Minor.	3. 6. 1. 1.
M. blackleri lycaon Thomas, 1919	*M. tristrami*	Kara Dagh, about 80 km, south-east of Konia, Lycaonia, Asia Minor.	8. 7. 1. 28
M. sacramenti Thomas, 1922	*M. sacramenti*	Ten miles south of Beersheba, Palestine	22. 10. 4. 1
Cheliones. h. collinus Thomas, 1919	*M. hurrianae*	Kohat, North-West Frontier Province, India.	7. 6. 8. 7
M. auceps Thomas, 1908	*M. meridianus*	East of Taiyuenfu, Shansi, China	8. 8. 7. 30.
Sekyytamys calurus Thomas, 1892	*S. calurus*	Near Tor, Sinai.	1988. 558.

2010; Boroni et al. 2017; Rey-Rodríguez et al. 2022). The use of landmark data to describe cranial and mandibular variation (both in size, and shape) is proven to be a sufficiently powerful tool in rodent systematics (Tabatabaei Yazdi and Adriaens 2013; Boroni et al. 2017; Rey-Rodríguez et al. 2021; Alhajeri 2020, 2021). Geometric morphometrics is a frequently used technique for the analysis of form based on Cartesian landmark coordinates (Bookstein 1991; Polly 2018). Landmarks are anatomically corresponding points digitized on each specimen. Differences in specimens' coordinates, due to rotation and translation of specimens, have removed by doing a procrustes' superimposition (Rohlf and Slice 1990). Size and shape components of form are analysed, separately. "Size", is measuring as centroid size (CS), the square root of the sum of squared distances between all landmarks and their centroid.

The landmark data were obtained from photographs taken with a Nikon D70 digital reflex camera using a Sigma 105 mm macro lens at five megapixels, through a standardized protocol. The landmark configuration adopted in the present study follows the ones in

Tabatabaei Yazdi et al. (2014, 2015). We digitized 21 ventral, 19 dorsal, and 21 lateral two-dimensional (2D) landmarks, using TpsDig2. (Fig. 1). For anatomical definition of the landmarks, based upon Popesko et al. (1992), see Table 2.

Analyses of shape and size

Before doing the shape analyses, we performed a Generalized Procrustes Analyses (GPA), using PAST software (PAlaeontologica STatistics) ver. 2.17 (Hammer et al. 2001). The patterns of shape variation have investigated based on Procrustes distances, following Bookstein (1991). Correctness of the projection of shape data, using TpsSmall ver. 1.34 (Rohlf 2004), was tested.

Principal component analysis (PCA) extracts singular vectors from the weight matrix. These singular vectors are equivalent to principal components (PCs). The scatter plots of the first two PCs were generated in STATISTICA (StatSoft 2004). The percentage of the variation that is explained by the PCs was calculated using PAST. For the first and second PCs the percentages are included in the corresponding graphs. The outlines representing shape variation explained by the PC axes, were generated using MorphoJ 1.07 (Klingenberg 2008).

TspSmall ver. 1.34 was used to obtain the average landmark configuration (consensus configuration) of each species. Procrust distances between each pair of OTU's (Operational Taxonomic Units) were calculated using TpsSmall (for ventral, dorsal, and lateral sides). The results are presented in Table 3.

In order to evaluate the overall pattern of morphometric similarities among the OTU's or their consensuses, UPGMA cluster analyses were performed. The analyses were done on the matrix of shape distances (Euclidean Distances) between the OTU's means, using PAST, and for each skull side, separately. The results of UPGMA were represented by dendograms, which were generated in PAST. The branch supports on the dendograms were estimated by performing a bootstrapping of 10,000 randomisations.

"Size" of the specimens have been computed as centroid size (CS). CS is the square root of the sum of squared distances of each landmark from the centroid of the landmark configuration of each specimen. The significance of the size differences among the OTU's was tested by ANOVA. Size differences were illustrated using the plots (Fig. 4). The significance of pairwise comparisons between the CS of the species was tested using the Tukey HSD test in STATISTICA ver. 12. Additionally, interlandmark distances between landmarks 7-8 on the ventral side (representing the length of teeth row), and landmarks 15-16 on the lateral side of skulls (representing the opening of suprameatal triangle, and the bulla inflation), were calculated in PAST. The obtained data were analysed using STATISTICA.

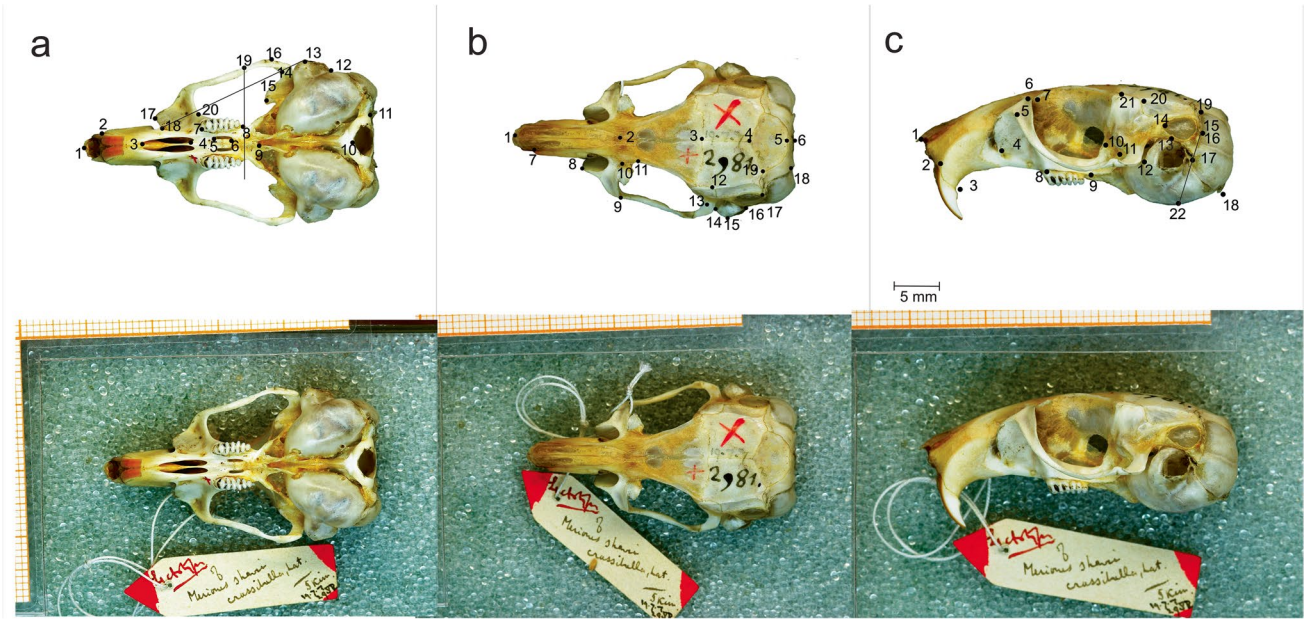

Fig. 1 Landmarks on the ventral (**a**), dorsal (**b**), and lateral (**c**) sides of *M. shawii* lectotype. The original photoghraphs bellow have been taken by the first author

Table 2 Description of the landmarks' position in this study (see Fig. 1)

Landmark	Definition
Ventral view	
1	rostral tip of internasal suture
2	most lateral junction point of incisive alveolus and body of premaxillary bone
3	most rostral point of incisive foramen
4	most caudal point of incisive foramen
5	most rostral point of palatine foramen
6	most caudal point of palatine foramen
7	most rostral point on the alveolus of the first molar
8	most caudal point on the alveolus of the third molar
9	most caudal point of median suture of palatine bone
10	most rostral point of foramen magnum
11	most lateral point of occipital condyle
12	most caudal point of acoustic tympanic bulla
13	rostral curvature point at level of the meatus
14	most caudal point of zygomatic process concavity formed by temporal bone
15	intersection between frontal squama, wing of presphenoid bone and wing of basisphenoid bone
16	most lateral point of zygomatic arch at maximum width of skull
17	rostral point of zygomatic plate
18	maximum curvature of zygomatic plate in infraorbital foramen
19	intersection of zygomatic arch and vertical line passing through most caudal point of third molar
20	intersection of the zygomatic plate and line connecting the landmarks 13 and 18
Dorsal view	
1	rostral tip of internasal suture
2	intersection of naso-frontal suture with the internasal suture
3	intersection of frontal-parietal suture and the interparietal suture
4	intersection of suture between left and right parietals, and parietal-interparietal suture
5	midline point of suture between interparietal and occipital
6	midline point of caudal margin of the occipital
7	most rostral point of suture between nasal and premaxilla
8	rostral end of zygomatic plate
9	most lateral point of zygomatic plate
10	lateral end of the maxillary-frontal suture
11	rostral point of upper orbital crest at level of interorbital depression
12	intersection of temporal line and suture between parietal and squamosal bones
13	tip of concavity of squamosal root of zygomatic arch
14	caudal tip of squamosal root of zygomatic arch
15	rostrolateral end of tympanic bulla convexity
16	caudal end of tympanic bulla on lateral edge of suprameatal process (supramastoid part of squamosal bone)
17	distal tip of lateral process of supraoccipital
18	caudal end of suture between the mastoid part of tympanic bulla and supraoccipital
19	intersection of parietal-interparietal and interparietal-occipital sutures
Lateral view	
1	most rostral point of nasal
2	inner extreme point of incisor at body of premaxillary bone
3	point at intersection between premaxillary and posterior end of incisive alveolus
4	most rostral end of infraorbital foramen edge on zygomatic plate
5	most ventral point at the margin of zygomatic plate
6	most caudal point of infraorbital foramen on zygomatic plate
7	most rostral point of suture between lacrimal and zygomatic plate
8	most rostral point of molar on alveolar process of maxilla

Table 2 (continued)

Landmark	Definition
9	most caudal point of molar on alveolar process of maxilla
10	most caudal point of optic canal
11	middle of alisphenoid canal
12	most caudal point of suture between jugal and squamosal root of zygomatic arch
13	intersection between rostral edge of tympanic bulla and most caudal point of gap between tympanic bulla and occipital process of temporal bone
14	rostral point of suprameatal triangle
15	lateral tip of supraoccipital process
16	tip of hamular process of temporal on suprameatal triangle
17	rostral end of suture between stylomastoid suture and stylomastoid foramen
18	most rostral point of paraoccipital process
19	intersection of suture between parietal and supraoccipital with suprameatal process of squamosa
20	intersection of temporal line and suture between parietal and squamosal
21	junction of suture between parietal and squamosal bone and suture between frontal and squamosal part of temporal bone
22	intersection of tympanic part of bulla and line connecting landmarks 16 and 17

Results

Shape

The PCA analyses show that in the ventral view, the PC1 clearly sets *M. crassus* and *M. libycus* apart from *M. tristrami* and *M. persicus* (Fig. 2). *Meriones libycus* partly overlapped with *M. shawii* in ventral, dorsal and lateral views (Fig. 2a, b, and c).

In the ventral view, *S. calurus*, is positioned just close to *M. c. charon*, and *M. syrius* (synonym of *M. libycus*). *M. sacramenti* is positioned between the *M. crassus* and *M. libycus*.

Visualisation of the shape differences by the transformation outlines, along the first PC, demonstrates that most of the shape changes are mainly occurring in the inflation of bulla (landmarks 11, 12, and 13, Fig. 2a), and forward-projection of nasal (landmark1, Fig. 2a).

The second PC mainly reflects differences in the convexity of zygomatic arch (landmarks 16 and 19).

For the dorsal shape, *M. crassus* and *M. libycus* are restricted to the higher range of PC1 (Fig. 2b), and they are perfectly apart from *M. tristrami* and *M. persicus*. *Meriones syrius* (synonym of *M. libycus*), is positioned in the middle range of PC1 scores. *Meriones sacramenti* shows morphological similarity with some synonyms of *M. crassus* (e.g, *palladus*, *pelerinus*, and *ismahelis*). The PC plot clearly sets *M. c. charon* and *M. c. longifrons* specimens, on the *M. libycus* specimens' polygon.

Meriones hurraianae is positioned in the middle of PC1 axis, and apart from the other OTU's. PC1 mainly represents variation in the braincase width, and PC2 mainly shows variation in the convexity of the zygomatic arch. The axes, demonstrate variation in the interparietal length and width (Fig. 2b).

Concerning the lateral shape, *M. tristrami* is the only one that does not overlap with any of the other species. *Meriones persicus* is partially overlapping with *M. rex*, as well. *Meriones shawii* is in the middle of morphospace, and shows considerable overlap with *M. libycus* (Fig. 2c). *Meriones shawii* and *M. rex* are apart, while they showed a fairly overlap in a ventral view. The location of *M. sacramenti* in morphospace is close to that of *M. l. schousboeii*. *S. calurus*, in this view is located apart from the *Meriones* species. Specimens belonging to *M. crassus* or *M. libycus* have distinctly higher PC1 scores, respecting a more inflated bulla and enlarged occiput (interlandmark 18-22, Fig. 2c). The second PC, in the lateral view mainly reflects variation in the skull length and position of the zygomatic process of the squamous part of the temporal bone that in some OTU's situated more caudally.

The pairwise comparisons of the Procrustes distances between the OTU's show that shape distances between specimens is similar to some degree for the three views (Table 3). However, different sides aren't equally informative.

The cluster analyses (UPGMA) on the ventral view data show that *M. tristrami* and *M. persicus* are most similar to each other (with higher bootstrap). These OTU's also clustered with *M. rex* and *M. shawii*. *M. crassus*, *M. libycus* and *M. sacramenti* are closest to each other. Interestingly, *S. calurus* shows more similarity with them (Fig. 3, Ventral).

The UPGMA, based on the dorsal view, shows that *M. crassus*, *M. libycus*, *M. shawii*, *M. sacramenti*, and *M.*

Table 3 Pairwise comparison of the studied OTU's based upon the procrust distances

Pairwise compared OTU's	Procrust distances between groups (Ventral)	Procrust distances between groups (Dorsal)	Procrust distances between groups (Lateral)
M. crassus-M. libycus	2.86E-02	3.07E-02	3.52E-02
M. crassus-M. persicus	6.96E-02	6.58E-02	8.33E-02
M. crassus-M. shawi	4.76E-02	3.61E-02	5.56E-02
M. crassus-M. rex	5.70E-02	5.96E-02	7.78E-02
M. crassus-M. tristrami	6.87E-02	7.35E-02	9.97E-02
M. crassus-M. sacramenti	3.24E-02	4.37E-02	5.83E-02
M. crassus-M. hurrianae	–	6.20E-02	7.34E-02
M. crassus-M. meridianus	5.97E-02	4.74E-02	6.89E-02
M. crassus-S. calurus	4.32E-02	6.56E-02	9.04E-02
M. libycus-M. persicus	5.70E-02	5.64E-02	7.02E-02
M. libycus-M. shawii	3.30E-02	2.73E-02	4.26E-02
M. libycus-M. rex	4.28E-02	4.78E-02	5.85E-02
M. libycus-M. tristrami	5.60E-02	6.46E-02	8.13E-02
M. libycus-M. sacramenti	3.43E-02	4.23E-02	5.38E-02
M. libycus-M. hurrianae	–	6.41E-02	5.98E-02
M. libycus-M. meridianus	5.89E-02	3.48E-02	6.10E-02
M. libycus-S. calurus	3.91E-02	5.27E-02	8.65E-02
M. persicus-M. shawii	3.66E-02	4.71E-02	4.26E-02
M. persicus-M. rex	4.65E-02	3.33E-02	4.40E-02
M. persicus-M. tristrami	2.66E-02	3.36E-02	4.34E-02
M. persicus-M. sacramenti	6.30E-02	6.96E-02	8.76E-02
M. persicus-M. hurrianae	–	6.66E-02	6.31E-02
M. persicus-M. meridianus	8.30E-02	5.72E-02	8.07E-02
M. persicus-S. calurus	5.81E-02	5.65E-02	7.26E-02
M. shawii-M. rex	3.79E-02	3.97E-02	3.95E-02
M. shawi-M. tristrami	3.39E-02	5.19E-02	5.73E-02
M. shawii-M. sacramenti	3.77E-02	3.97E-02	5.75E-02
M. shawii-M. hurrianae	–	5.92E-02	4.93E-02
M. shawii-M. meridianus	6.71E-02	3.89E-02	6.89E-02
M. shawii-S. calurus	4.39E-02	5.03E-02	7.89E-02
M. rex-M. tristrami	4.06E-02	3.87E-02	5.36E-02
M. rex-M. sacramenti	5.03E-02	6.58E-02	7.87E-02
M. rex-M. hurrianae	–	5.79E-02	5.30E-02
M. rex-M. meridianus	7.19E-02	5.18E-02	6.12E-02
M. rex-S.calurus	5.22E-02	3.47E-02	9.08E-02
M. tristrami-M. sacramenti	6.01E-02	7.83E-02	1.06E-01
M. tristrami-M. hurrianae	–	7.56E-02	6.69E-02
M. tristrami-M. meridianus	7.62E-02	6.28E-02	8.98E-02
M. tristrami-S. calurus	5.68E-02	5.12E-02	8.65E-02
M. sacramenti-M. hurrianae	–	6.77E-02	8.61E-02
M. sacramenti-M. meridianus	5.66E-02	5.73E-02	8.72E-02
M. sacramenti-S. calurus	4.62E-02	7.44E-02	1.15E-01
M. hurrianae-M. meridianus	–	6.46E-02	7.48E-02
M. hurrianae-S. calurus	–	7.20E-02	9.19E-02
M. meridianus-S. calurus	6.20E-02	5.37E-02	1.03E-01

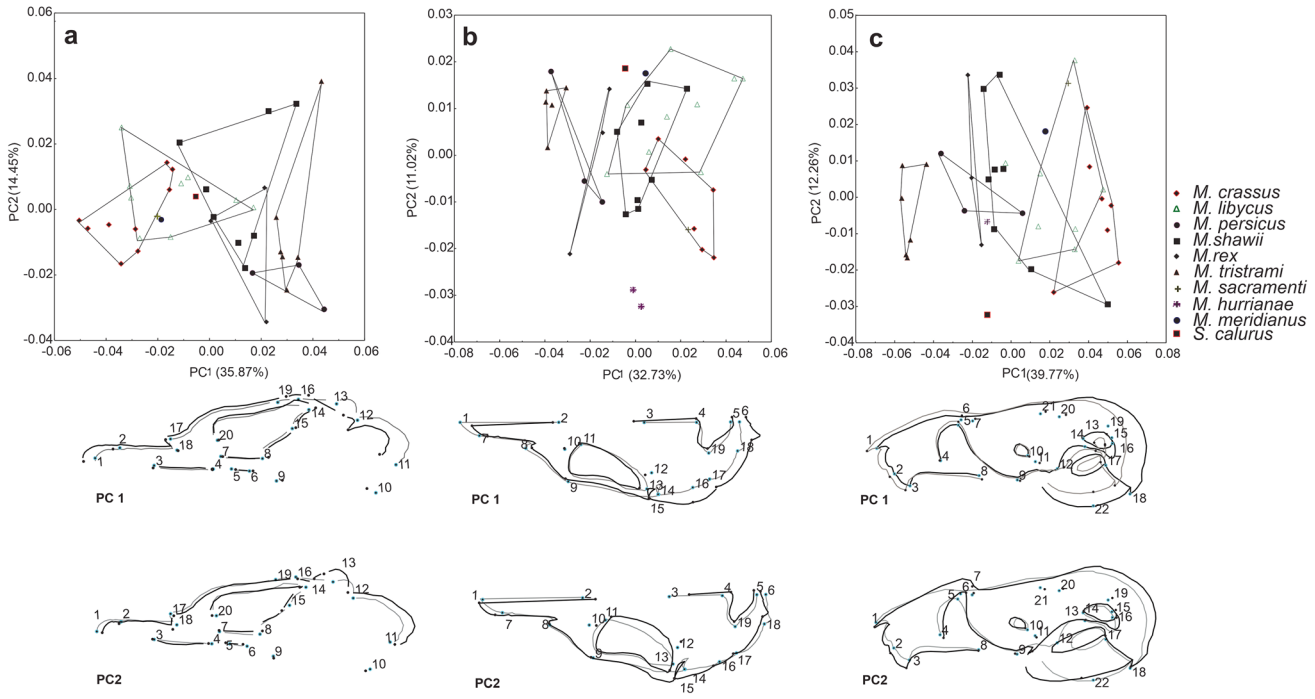

Fig. 2 Scatter plot of PCA results on shape variables of ventral (**a**), dorsal (**b**), and lateral (**c**) sides of specimens. Outlines show shape transformations along the axes (from grey to black)

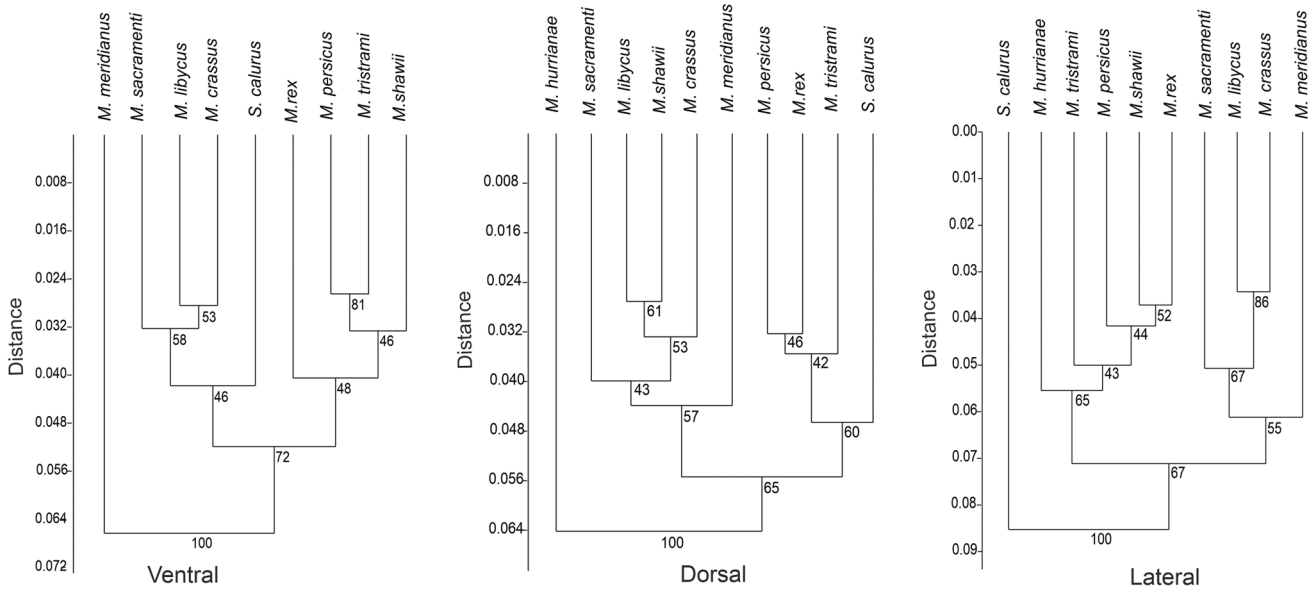

Fig. 3 Dendograms obtained from the UPGMA on the ventral, dorsal and lateral views' shape data, using Euclidean distances between OUT's means (branch bootstrap support shown as percentage at the nodes, 10,000 replicates). Nodes with lower bootstrap could be affected by low sampling

meridianus were clustered together. *M. tristrami*, *M. rex*, *M. persicus*, and *S. calurus* were clustered together (Fig. 3, Dorsal).

With respect to lateral dataset, *S. calurus*, corroborating the PC results, is partly apart. *M. crassus*, *M. libycus*, *M. sacramenti* and *M. meridianus* cluster together. *M. crassus* and *M. libycus*, with higher bootstrap, are the closest OTU's. *Meriones shawii*, in contract with dorsal view, clustered with *M. tristrami*, *M. rex*, *M. persicus*, and *M. hurrianae* (Fig. 3, Lateral).

Size

There is a significant size difference (F = 3.3603, $p < 0.01$) among the species' centroid size (CS). Since sexual dimorphism didn't influence the observed species differences ($F_{sex*species} = 0.8$, $p = 0.51$), both sexes are grouped. *Meriones persicus* has the largest, and *M. meridianus*, has the smallest crania (Fig. 4a). Tukey HSD test on centroid size dataset shows a significant difference between *M. crassus* and *M. persicus*. *Meriones meridianus* has significantly smaller cranium than *M. persicus*, *M. rex*, and *M. sacramenti*. Although, *M. crassus* has larger mean of CS than *M. libycus*, these species are not significantly different.

A significant difference (F = 7.9992, $p < 0.01$) was among the species, based on the distance between landmarks 7-8 (Fig. 4b). This distance, representing tooth row length, was maximum in *M. rex* and *M. persicus*, respectively. It was minimum in *M. meridianus* and *S. calurus* (Fig. 4b). The results of a Tukey HSD test on dataset corresponding tooth row length (i.e. landmarks 7- 8), show significant differences ($p < 0.01$) between the following pairs: *M. crassus* and *M. persicus*, *M. crassus* and *M. rex*, *M. libycus* and *M. rex*, and *M. tristrami* and *M. rex*. Regarding this criteria, remarkably *S. calurus* shows more similarity with *M. crassus*, and *M. meridianus*.

Regarding the analysis of the inter-landmarks' distances between landmarks 15 and 16, a significant difference (F = 4.2511, $p < 0.01$) was found among the species. This distance was maximum in *M. crassus* and *M. sacramenti,* respectively. The closest suprameatal triangle was observed in *M. tristrami* and *S. calurus* (Fig. 4c). The results of Tukey HSD test show significant differences ($p < 0.01$) between the following pairs: *M. hurrianae* and *S. calurus*, and between *M. crassus* and *M. tristrami.*

Discussion

The results (i.e. the cluster analyses) demonstrate that the OTU's are clustering into two main groups, mainly based on the relative tympanic bulla size. Patterns of variation in bulla size have already been described for some jird species (Tabatabaei Yazdi and Adriaens 2013). Intraspecific variation in bulla size has been observed in *M. meridianus*, *M. crassus*, *M. tristrami* and *M. libycus* (Tabatabaei Yazdi and Adriaens 2013; Tabatabaei Yazdi et al. 2014, 2015). Such morphological plasticity reflects differences in climatological conditions. In other words, since the hearing ability is associated with larger bullae, having a larger bulla is a biological advantage for living in xeric environments (Pavlinov and Rogovin 2000; Harrison 1972; Vaughan et al. 2000; Alhajeri 2019). Concerning the ventral and dorsal skull shape, *M. tristrami* and *M. persicus* demonstrate a partly overlapping in the morphospace, while in the lateral shape *M. tristrami* is apart, without any overlapping in the morphospace.

Concerning *M. blackleri*, currently a synonym of *M. tristrami*, we observed more morphological similarity (i.e. in the dendograms) between *M. blackleri* and *M. persicus*, than with *M. tristrami.* These results that reflect aspects of cranial similarities, such as bulla inflation, are in agreement with Yigit et al. (2006), Darvish (2011), and Tabatabaei Yazdi and Adriaens (2013).

Regarding *M. sacramenti*, the results (i.e., PCA), show that in the ventral view, this species is similar to *M. schousboei* (*M. libycus*), in the dorsal view is similar to *M. gaetulus* (*M. libycus*), and in the lateral view is similar to *M. ismahelis* (*M. crassus*). Additionally, we should mention that *M. sacramenti* is a rare and endangered species (IUCN 2016) with a small range of distribution (Israel/Palestine). This species, in the past, was a closely related taxon to *M. shawii* and *M. libycus* (Musser and Carleton 2005; Darvish 2011). So, a study with a multi-disciplinary approach (including advanced molecular, morphological, and ecological), is needed to clarify the taxonomy of this taxon and other sympatric taxa in synonymy with *M. tristrami* Thomas 1892.

Our results generally show that *M. shawii* has considerable similarities with *M. libycus*, especially subspecies as *auratus* and *arimalius*. We should mention that *auratus*, based upon our shape data (weight matrix of all sides of a skull), shows overlap with the polygon of other *M. shawii* synonyms. *M. shawii*, showing a morphological overlap in the morphospace (PCA) with *M. libycus*, was previously discussed by Zaime and Pascal (1988) in Happold (2013). These authors have discussed about the craniometrical similarities of these OUT's. *Meriones shawii* was listed as the synonym of *M. libycus*, in past (old ver. Musser and Carleton 2005). Identification of *M. shawii* and *M. libycus* is often confusing in the museum collections and so doubtful in the published reviews and reports on *Meriones* (Musser and Carleton 2005). We should mention that in the dorsal and lateral views, less similarity was observed between *M. shawii* and *M. tristrami*, rather than in the ventral view.

Meriones auratus, which was regarded as the synonym with *M. libycus* by Musser and Carleton (2005), currently is listed as the synonym of *M. shawi*, in the latest version of this reference. Based on our results, *M. auratus* is morphologically similar to *M. albipes*, which is in synonymy with *M. shawii.*

Meriones arimalius (Arabian jird) from central Arabia, in synonymy with *M. libycus*, show morphological similarity with some synonyms of *M. libycus* and *M. crassus.* In ventral view, it is similar to *schousboei* (synonym of *M. libycus*), and then *palidus* (synonym of *M. crassus*). In the dorsal view is close to *gaetulus* (synonym of *M. libycus*),

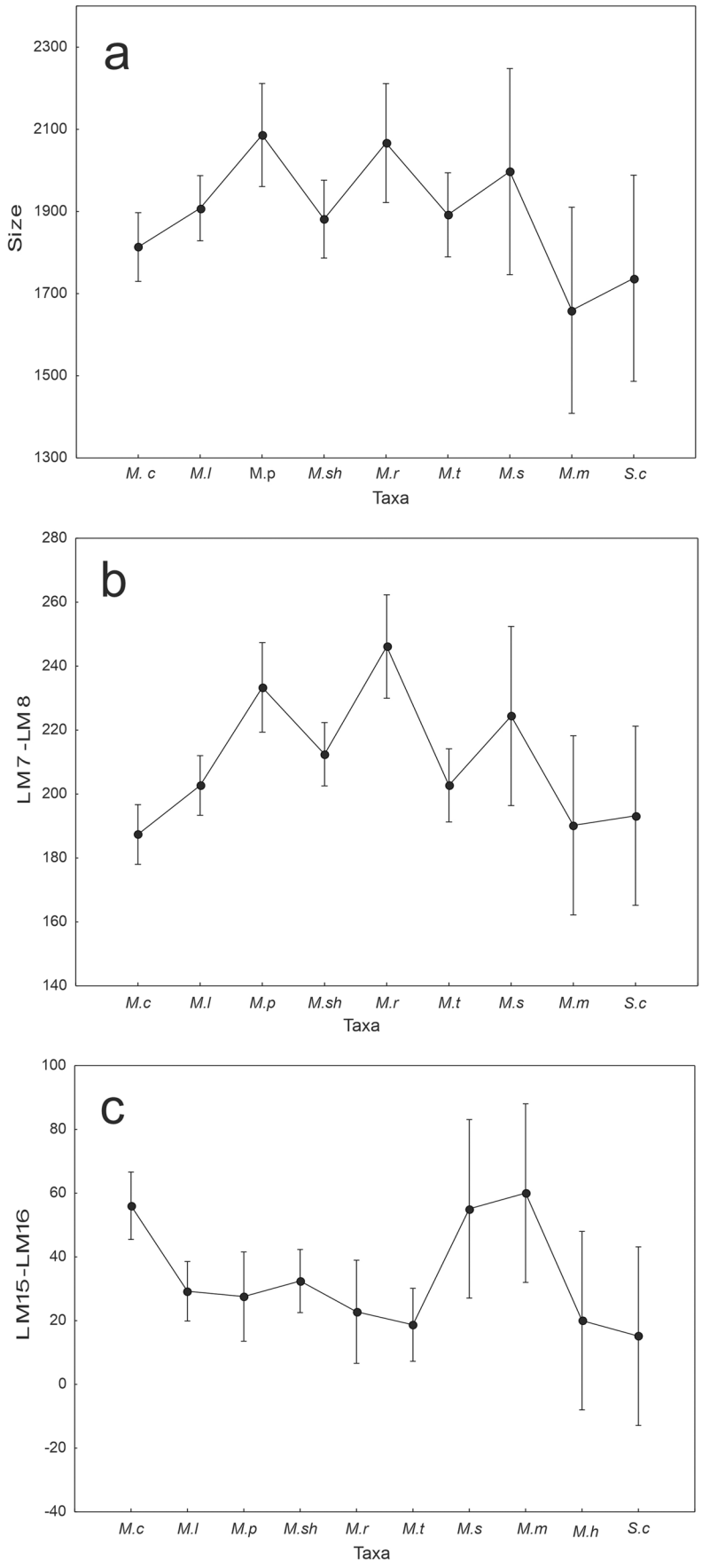

Fig. 4 Plots showing means of the centroid sizes (c, calculated based on the ventral configurations), distances between landmarks 7-8 (**b**), and 15-16 of each species (**c**). Wiskers represent SE

and in the lateral view, is similar to *ismahelis* and *palidus* (synonym of *M. crassus*).

In agreement with Darvish (2011), *M. arimalius* shows morphological similarity with both *M. libycus*, and *M. crassus*. Therefore, it needs a complete systematic revision.

Meriones syrius (synonym of *M. libycus*), showing cranial morphological similarity to *M. shawii* and *longifrons* (synonym of *M. crassus*) and which share burrows with sympatric *M. syrius*, may imply the need for a more thorough and entire revision of these sympatric taxa, moreover than focusing on potential hybridisation between them.

Our results show considerable similarity in cranial morphology between *charon* (subspecies of *M. crassus*, from Khuzestan plain and Mesopotamia), and *M. l. syrius*, and also between *M. e. caucasius* (synonym of *M. libycus*), and *M. erythrourus* (synonym of *M. crassus*). Both Heptner (1940), and Ellerman (1948) reported the occurrence of *M. erythrourus* (*M. e. caucasius*) in Khuzestan province. Thus, the specimens collected from this locality might be identified as the synonym of either *M. libycus* or *M. crassus.*

According to results obtained by multivariate analyses in this study and our previous investigations on the genus *Meriones* (Alhajeri et al. 2015; Dianat et al. 2020), we may conclude that the similarities in cranial morphology among the genus *Meriones*, in addition to phylogeny is noticeably linked to the climatic conditions. The *Meriones* species show considerable morphological plasticity and have evolved related to habitat conditions. This fact has been well discussed in the past (Tabatabaei Yazdi 2011; Tabatabaei Yazdi and Adriaens 2013; Tabatabaei Yazdi et al. 2014). Alhajeri (2019) and Abiadh et al. (2010) proposed the same hypothesis for Gerbillinae, as well.

The size analyses on the different datasets demonstrated that distances between landmarks 7-8 on the ventral view (i.e. the length of teeth row) were significantly different between some jird species. Thus, this metric distance could be of interest to taxonomists. In contrast, distances between landmarks 15-16 on the lateral view that shows a noticeable intra-species variation, indubitably is unusable in the species identification.

Regarding the conservation context, the status of some *Meriones* species in IUCN is "Endangered", i.e. *M. sacramenti, M. arimalius*, and *M. dahli.* Most of the jirds are in the status of "Lower Risk", e.g., *M. hurrianae*, *M. libycus, M. meridianus*, and *M. crassus*. At a glimpse, the species with limited distribution range have listed as the endangered species. Some of these OUT's are cryptic species, and several times have reinstated. Most of jird species are complex (Tabatabaei Yazdi et al. 2012), and include locally endangered populations that have not been defined or well appreciated.

As we mentioned before, the taxonomy of *Meriones* is complicated. One of the major causes of this mixed-up taxonomy in this genus is taxonomical identification based on some morphological traits that show a variation at the level of intra-species. Therefore, the diagnostic criteria should be defined after eagle-eyed the inter-specific morphological variation.

Concussively, only a thorough systematic revision of the genus *Meriones*, including zoogeographic and ecological data, may complete the puzzle of the taxonomy of these species.

Appendix

Collection numbers of the studied specimens at the British Museum of Natural History (London, UK).

Meriones crassus Sundevall, 1842

5. 10. 4. 38, 24. 8. 2. 4, 10. 3. 12. 5, 2. 11. 4. 64, 83. 11. 30. 1, 19. 7. 7. 2246.

Meriones libycus Lichtenstein, 1823

24. 8. 2. 5., 12. 4. 1. 44., 82. 7. 29. 9, 2. 11. 4. 56, 25. 5. 12. 59, 19. 7. 7. 1560, 5. 7. 2. 2, 24. 8. 2. 6., 24. 8. 2. 7.

Meriones persicus Blanford, 1875

5. 10. 4. 35, 76. 3. 10. 2, 19. 11. 7. 69.

Meriones shawii (Dovernoy, 1842)

19. 7. 7.1567, 82. 7. 29. 10., 82. 7. 29. 8., 92. 7. 1. 6, 19. 7. 7. 2981, 19. 7. 7. 1941, 82. 7. 29. 7.

Meriones rex Yerbury and Thomas, 1895

2. 11. 22. 9, 40. 272, 95. 6. 1. 30

Meriones tristrami Thomas, 1892

3. 6. 1. 1., 8. 7. 1. 28

Meriones sacramenti Thomas, 1922

22. 10. 4. 1

Meriones hurrianae Jordan, 1867

7. 6. 8. 7

Meriones meridianus (Pallas, 1773)

8. 8. 7. 30.

Sekeetamys calurus (Thomas, 1892)

1988. 558.

Acknowledgments We are very grateful to all museum curators and collection managers who provided us with access to the collections. Thanks to anonymous referees for their helpful comments that improved the quality of the manuscript.

Authors' contribution Both authors contributed equally in all aspects of this study and both approved the final manuscript.

Data availability The datasets generated during and/or analysed during the current study are available from the corresponding author on reasonable request.

Declarations

All authors have read and agreed to the submitted version of the manuscript.

Ethical approval Ethical approval is not required for the studied specimens.

Conflict of interest The authors declare no conflict of interest.

References

Abiadh A, Colangelo P, Capanna E, Lamine-Cheniti T, Chetoui M (2010) Morphometric analysis of six *Gerbillus* species (Rodentia, Gerbillinae) from Tunisia. C R Biol 333:687. https://doi.org/10.1016/j.crvi.2010.07.003

Alhajeri BH (2019) Cranial variation in geographically widespread dwarf gerbil *Gerbillus nanus* (Gerbillinae, Rodentia) populations: isolation by distance versus adaptation to local environments. J Zool Syst Evol 57:191–203. https://doi.org/10.1111/jzs.12247

Alhajeri BH (2020) A geometric morphometric analysis of geographic mandibular variation in the dwarf gerbil, *Gerbillus nanus* (Gerbillinae, Rodentia). J Mamm Evol 28:1–12. https://doi.org/10.1007/s10914-020-09530-9

Alhajeri BH (2021) A geometric morphometric analysis of geographic mandibular variation in the dwarf gerbil *Gerbillus nanus* (Gerbillinae, Rodentia). J Mamm Evol 28:469–480. https://doi.org/10.1007/s10914-020-09530-9

Alhajeri BH, Hunt OJ, Steppan SJ (2015) Molecular systematics of gerbils and deomyines (Rodentia: Gerbillinae, Deomyinae) and a test of desert adaptation in the tympanic bulla. J Zool Syst Evol 53:312–330. https://doi.org/10.1111/jzs.12102

Bookstein FL (1991) Morphometric tools for landmark data. Cambridge University Press, New York

Boroni L, Lobo N, Romano LS, Romano PSR, Lessa G (2017) Taxonomic identification using geometric morphometric approach and limited data: an example using the upper molars of two sympatric species of *Calomys* (Cricetidae: Rodentia). Zoologia 34:1–11. https://doi.org/10.3897/zoologia.34.e19864

Cardini A, Elton S (2009) The radiation of red colobus monkeys (Primates, Colobinae): morphological evolution in a clade of endangered African primates. Zool J Linnean Soc 157:197–224

Cardini A, Jansson A, Elton S (2007) Ecomorphology of vervet monkeys: a geometric morphometric approach to the study of clinal variation. J Biogeogr 34:1663–1678

Cardini A, Diniz Filho JAF, Polly PD, Elton S (2010) Biogeographic analysis using geometric morphometrics: clines in skull size and shape in a widespread African arboreal monkey. In: Elewa A (eds) Morphometrics for Nonmorphometricians. Lecture Notes in Earth Sciences, vol 124. Springer, Berlin, Heidelberg, pp 191–217

Chaworth-Musters JL, Ellerman JR (1947) A revision of the genus *Merioes*. Proc Zool Soc Lond 117:478–504. https://doi.org/10.1111/j.1096-3642.1947.tb00533.x

Chevret P, Dobigny G (2005) Systematics and evolution of the subfamily Gerbillinae (Mammalia, Rodentia, Muridae). Mol Phylogenet Evol 35:674–688. https://doi.org/10.1016/j.ympev.2005.01.001

Darvish J (2009) Morphmetric comparison of fourteen species of the genus *Meriones* Illiger, 1811 (Gerbillinae, Rodentia) from Asia and North Africa. Iran Anim Biosyst (IJAB) 5:59–77

Darvish J (2011) Morphological comparison of fourteen species of the genus *Meriones* Illiger, 1811 (Rodentia: Gerbillinae) from Asia and North Africa. Iran Anim Biosyst (IJAB) 7:50–72. https://doi.org/10.22067/ijab.v7i1.25506

Dianat M, Darvish J, Aliabadian M, Siahsarvie R, Krystufek B, Nicolas V (2020) Systematics and evolution of the Libyan jird based on molecular and morphometric data. J Zool Syst Evol 58:439–458. https://doi.org/10.1111/jzs.12335

Ellerman J (1948) Key to the rodents of south-West Asia in the British museum collection. Proc Zool Soc Lond: 765-816. https://doi.org/10.1111/j.1096-3642.1948.tb00406.x

Fadda C, Corti M (2001) Three-dimensional geometric morphometrics of *Arvicanthis*: implications for systematics and taxonomy. J Zool Syst Evol 39:235–245. https://doi.org/10.1046/j.1439-0469.2001.00169.x

Hammer Ø, Harper DA, Ryan PD (2001) PAST: paleontological statistics software package for education and data analysis. Palaeontol Electron 4:9

Happold DCD (2013) Mammals of Africa. Volume 3: Rodents, Hares and Rabbits. Bloomsbury Publishing, London, pp 27-691

Harrison DL (1972) The mammals of Arabia: Lagomorpha; Rodentia. Benn, London, pp 382–670

Heptner WG (1940) [The gerbilline fauna of Iran, withzoogeographic peculiarities of Anatolia, Iran, Afghan regions]. Novye Memuary MOIP. Vol. 20, pp 171. [InRussian]

IUCN (2016) The IUCN Red List of Threatened Species, Version 2021–3. http://www.iucnredlist.org/. Accessed Sept 2021

Klingenberg C (2008) Morphological integration and developmental modularity. Annu Rev Ecol Evol Syst 39:115–132. https://doi.org/10.1146/annurev.ecolsys.37.091305.110054

Macholán M, Mikula O, Vohralík V (2008) Geographic phenetic variation of two eastern-Mediterranean non-commensal mouse species, *Mus macedonicus* and *M. cypriacus* (Rodentia: Muridae) based on traditional and geometric approaches to morphometrics. Zool Anz 247:67–80. https://doi.org/10.1016/j.jcz.2007.07.003

Mahmoodzadeh A, Eisapoor SS, Mirghiasy SA (2022) Biodiversity in the third millennium. Sci Rep Life Sci 3(2):1–14. https://doi.org/10.5281/zenodo.6840509

Musser GG, Carleton, MD (2005) Superfamily muroidea. In: Wilson DE, Reeder DM (eds) Mammal species of the world: a taxonomic and geographic reference. The Johns Hopkins University Press, Baltimore, p 2142

Pavlinov IY (2008) A review of phylogeny and classification of Gerbillinae (Mammalia: Rodentia). University Publishing Moscow, Moscow

Pavlinov II, Rogovin K (2000) The correlation of the size of the pinna and the auditory bulla in specialized desert rodents. Zh Obshch Biol 61:87–101

Polly PD (2018) Geometric morphometrics. In: López-Varela SL (ed) The SAS encyclopedia of archaeological sciences, John Wiley & Sons, Inc., Oxford. p. 1–5. https://doi.org/10.1002/9781119188230.saseas0258

Popesko P, Rajtovaa V, Horaak J (1992) A colour atlas of the anatomy of small laboratory animals. Saunders Ltd, London

Rey-Rodríguez I, Arnaud J, López-García J-M, Stoetzel E, Denys C, Cornette R, Bazgir B (2021) Distinguishing between three modern *Ellobius* species (Rodentia, Mammalia) and identification of fossil *Ellobius* from Kaldar cave (Iran) using geometric morphometric analyses of the first lower molar. Palaeontol Electron 24(1):1–18. https://doi.org/10.26879/1122

Rey-Rodríguez I, Arnaud J, López-García J-M, Stoetzel E, Denys C, Arnaud J, Parfitt S, Fernández-Jalvo Y, King T (2022) Palaeoecological reconstructions of the middle to Late Pleistocene occupations in the southern Caucasus using rodent assemblages. Archaeol Anthropol Sci 14(5):96. https://doi.org/10.1007/s12520-022-01555-w

Rohlf FJ (1996) Morphometric spaces, shape components and the effects of linear transformations. In: Marcus LF, Corti M, Loy A, Naylor GJP, Slice DE (eds) Advances in Morphometrics. NATO ASI Series, vol 284. Springer, Boston, MA, pp 117–129

Rohlf FJ (2004) TPS series. Department of Ecology and Evolution, State University of New York, Stony Brook

Rohlf FJ, Slice D (1990) Extensions of the Procrustes method for the optimal superimposition of landmarks. Syst Biol 39:40–59. https://doi.org/10.2307/2992207

StatSoft, Inc. (2004). STATISTICA (data analysis software system), version 12. www.statsoft.com. Accessed Sept 2021

Stoetzel E, Cornette R, Lalis A, Nicolas V, Cucchi T, Denys C (2017) Systematics and evolution of the *Meriones shawii/grandis* complex (Rodentia, Gerbillinae) during the Late Quaternary in northwestern Africa: exploring the role of environmental and anthropogenic changes. Quat Sci Rev 164:199–216. https://doi.org/10.1016/j.quascirev.2017.04.002

Tabatabaei Yazdi F (2011) Patterns of variation in skull phenotypes in *Meriones* (Rodentia: Muridae) from the Iranian region, in relation to species and environmental-geographical diversity. Ghent University. Faculty of Sciences, Ghent, Belgium. https://hdl.handle.net/1854/LU-1270182

Tabatabaei Yazdi F (2017) Testing and quantification of cranial shape and size variation within *Meriones hurrianae* (Rodentia: Gerbillinae): a geometric morphometric approach. Mammalia 87:160–167. https://doi.org/10.1016/j.mambio.2017.08.004

Tabatabaei Yazdi F, Adriaens D (2013) Cranial variation in *Meriones tristrami* (Rodentia: Muridae: Gerbillinae) and its morphological comparison with *Meriones persicus*, *Meriones vinogradovi* and *Meriones libycus*: a geometric morphometric study. J Zool Syst Evol 51:239–251. https://doi.org/10.1111/jzs.12020

Tabatabaei Yazdi F, Adriaens D, Darvish J (2012) Geographic pattern of cranial differentiation in the Asian midday Jird *Meriones meridianus* (Rodentia: Muridae: Gerbillinae) and its taxonomic implications. J Zool Syst Evol 50:157–164. https://doi.org/10.1111/j.1439-0469.2011.00642.x

Tabatabaei Yazdi F, Adriaens D, Darvish J (2014) Cranial phenotypic variation in *Meriones crassus* and *M. libycus* (Rodentia, Gerbillinae), and a morphological divergence in *M. crassus* from the Iranian plateau and Mesopotamia (Western Zagros Mountains). Eur J Taxon 88:1–28. https://doi.org/10.5852/ejt.2014.88

Tabatabaei Yazdi F, Colangelo P, Adriaens D (2015) Testing a long-standing hypothesis on the relation between the auditory bulla size and environmental conditions: a case study in two jird species (Muridae: *Meriones libycus* and *M. crassus*). Mammalia 79:185–200. https://doi.org/10.1515/mammalia-2013-0043

Vaughan TA, Ryan JM, Czaplewski NJ (2000) Mammalogy, 4th edn. Harcourt College Publisher, New York

Wilson DE, Reeder DM (2005) Mammal species of the world: a taxonomic and geographic reference. JHU Press, Baltimore

Wrobel M (2006) Elsevier, dictionary of mammals. Elsevier

Yigit N, Gharaheloo MM, Çolak E, Özkurt Ş, Bulut Ş, Kankiliç T, Çolak R (2006) The karyotypes of some rodent species (Mammalia: Rodentia) from eastern Turkey and northern Iran with a new record, *Microtus schidlovskii* Argyropulo, 1933, from eastern Turkey. Turk J Zool 30:459–464

Zelditch ML, Swiderski DL, Sheets HD, Fink WL (2004) Geometric morphometrics for biologists: a primer. pp 1–20. https://doi.org/10.1016/B978-012778460-1/50003-X